Single- and Two-Phase Turbulent Mixing Rate between Subchannels in Triangle Tight Lattice Rod Bundle*

Akimaro KAWAHARA**, Michio SADATOMI**, Hiroyuki KUDO** and Keiko KANO**

In order to obtain the data on turbulent mixing rate between triangle tight lattice subchannels, which will be adopted as the next generation BWR fuel rod bundle, adiabatic experiments were conducted for single- and two-phase flows under hydrodynamic equilibrium flow conditions. The gas and liquid mixing rates measured for two-phase flows were found to be affected by the void fraction and/or flow regime, as reported in our previous study on a simulated square lattice rod bundle channel having hydraulic diameters of about four times larger than the present tight lattice channel. Comparing the present mixing rate data with those for the square lattice channel and a triangle one in other institution, we found that the mixing rate was considerably smaller in the present channel than the other ones, i.e., a channel size effect.

Key Words: Nuclear Reactor, Multi-Phase Flow, Turbulent Mixing, Subchannel Analysis, Tight Lattice Rod Bundle, Single-Phase Flow, Two-Phase Flow

1. Introduction

As a next generation nuclear reactor, a high-conversion BWR is planning[1]. A higher conversion ratio is anticipated by narrowing the flow area among the fuel rods in the reactor since the moderation of neutron decreases with the area. In the fuel assembly, therefore, a triangle tight lattice array of the rods is planning, and the spacing between the rods will be narrowed to about 1 mm to get a conversion ratio higher than unity. In the development of such a reactor, an accurate prediction of a critical power is essential because the deterioration of cooling performance is apprehended compared with a conventional BWR fuel rod bundle. For predicting the critical power in a conventional BWR fuel rod bundle, a subchannel analysis code is usually used. In addition, the use of the code is under consideration also for a tight lattice fuel rod bundle. However, there are few experimental data on such a bundle to validate the code, especially the data on an inter-subchannel fluid transfer, which is one of key parameters in the subchannel analysis.

The fluid transfer in a gas-liquid two-phase flow system has been modeled as three independent components; turbulent mixing, void drift and diversion cross-flow[2),(3)]. Therefore, we started an experimental program for studying each fluid transfer component between tight lattice subchannels[4),(5)]. In the program, a newly constructed test channel, consisted of two vertical subchannels simplifying a triangle tight lattice rod bundle, has been used.

In this study, using the above mentioned channel, we obtained the data on the turbulent mixing rate between the subchannels as well as the void fraction for single- and two-phase air-water flows under hydrodynamic equilibrium flow conditions, i.e., in the absence of both the void drift and the diversion cross-flow. Furthermore, correlations and models of the turbulent mixing rate in literatures have been tested against the present data. Regarding the prediction of the single-phase mixing rate, a new correlation has been developed based on the present data as well as available data for triangle lattice rod bundle channels. Results of such experiments and tests are described in this paper.

2. Experiments

2.1 Test channel

Figure 1 shows the cross-section of the test channel. The channel consisted of two identical subchannels, each surrounded by four partial rods in a triangular array. The

* Received 9th September, 2005 (No. 05-4158)

** Department of Mechanical System Engineering, Graduate School of Science and Technology, Kumamoto University, 2–39–1 Kurokami, Kumamoto-city, Kumamoto 860–8555, Japan.
E-mail: akimaro@mech.kumamoto-u.ac.jp;
sadatomi@mech.kumamoto-u.ac.jp;
keiko@mech.kumamoto-u.ac.jp

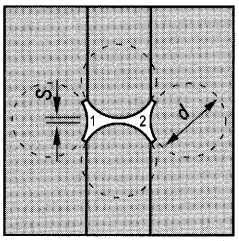

Gap clearance: S = 1.0 mm
Rod diameter: d = 12.0 mm
Rod to rod pitch: p = 13.0 mm
Pitch/rod diameter: p/d = 1.083
Hydraulic diameter: D_h = 3.19 mm
Flow area of one subchannel: A_1 = 16.6 mm^2

Fig. 1 Cross-section of the test channel

rod diameter, d, and the rod-to-rod pitch, p, were 12.0 mm and 13 mm, so the pitch to the rod diameter ratio, p/d, was 1.083. The gap clearance between the rods, S, was 1.00 ±0.02 mm. The hydraulic diameter, D_h, and the cross-sectional area of the subchannel, A_i, were 3.19 ±0.06 mm and 16.6 ±0.3 mm^2. These are about a quarter and one-eighth of those of the center subchannel in a typical BWR. In order to get hydraulically smooth inner walls and to observe a flow, the test channel was machined from transparent acrylic slabs and polished quite well.

2.2 Test rig and method

Figure 2 shows the flow loop of the test apparatus. Water and air at an atmospheric pressure and at a room temperature were used as the working fluids. The flow loop was mainly divided into three sections, entry (#1, 0.31 m in length), test (#2, 1.6 m) and discharge (#3, 0.31 m) sections from the bottom to the top. In the entry and the discharge sections, as seen in the left side of Fig. 2, a 1 mm thick partition inserted in the gap portion completely blocked the movement of the fluids between the subchannels. Therefore, the inter-subchannel fluid transfer could occur only in the test section.

After measuring the gas and liquid flow rates at the inlet of the respective subchannels with calibrated rotameters (#5) and positive displacement flowmeters (#4), the fluids were introduced into the respective subchannels from mixers (#6). In order to set a hydrodynamic equilibrium flow in the test section, the flow rate of each phase introduced into each subchannel had to be the same between the subchannels. At the inlet of the discharge section, the pressure difference between the subchannels was minimized in order to realize isokinetic discharge. This was done by controlling the openings of the respective air discharge valves connected to two separator rooms (#7). The accuracy of the flow rates measurement was confirmed to be 1% for water and 3% for air from the calibration of the flowmeters.

After setting the equilibrium flow, the turbulent mixing rate of k-phase ($k = G$ for gas, $k = L$ for liquid) between the subchannels, W'_k, were measured with a tracer technique[6]. Firstly, the respective tracers (methane for the gas phase and acid orange II water solution for the liquid phase) were injected into one of the two subchannels from a position upstream of the flow meters. Small

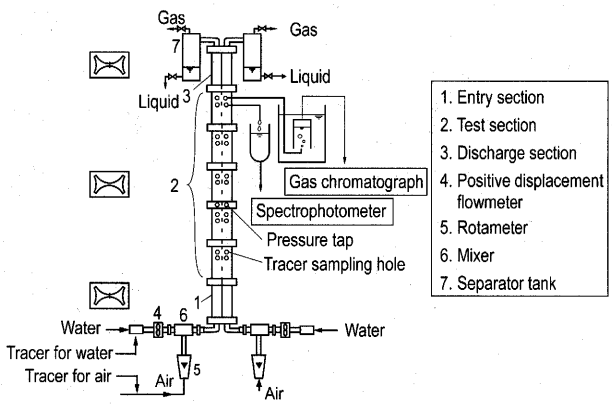

Fig. 2 Test apparatus

amounts of gas and liquid containing the tracers were extracted from four different axial positions in each subchannel in the test section. The concentrations of tracers in the fluids extracted were measured within an accuracy of 3% with a calibrated gas chromatograph for the gas phase and within 1.5% with a calibrated spectrophotometer for the liquid phase. As a result, the axial concentration profile for the each phase tracer was obtained. Finally, we could determine the turbulent mixing rate, W'_k, by fitting the concentration data to the following equation[6]:

$$W'_k = \frac{G_{k1}A_1 \cdot G_{k2}A_2}{\Delta Z(G_{k1}A_1 + G_{k2}A_2)} \times \ln\left\{\frac{C_{k1}(Z) - C_{k2}(Z)}{C_{k1}(Z+\Delta Z) - C_{k2}(Z+\Delta Z)}\right\}. \quad (1)$$

Here, G_{k1} is the k-phase mass velocity in subchannel 1 (Ch.1 for short), $C_{k1}(Z)$ the k-phase tracer concentration in Ch.1 at an axial position Z, A_1 the cross-sectional area of Ch.1, and ΔZ the distance between two axial positions.

We injected the tracer fluid alternately into each subchannel and confirmed that the turbulent mixing rates obtained for both cases agreed within 8%. From this reproducibility and from the accuracy of the measurements of tracer concentrations and flow rates, the probable error of W'_k was estimated. The resulting error was within ±15% for single-phase flow and both phases in two-phase bubble and annular flows, and within ±25% for the liquid phase and ±40% for the gas phase in two-phase slug or churn flow.

In addition to measurement of the turbulent mixing rate, mean void fraction was measured with the well-known quick shut valve method. The paired valves, 300 mm apart each other, were installed in the middle of the test section. The valves were simultaneously closed with solenoids very quickly within 0.1 second. In order to obtain accurate void fraction data within ±0.1%, the operation were repeated 10 to 20 times depending on the flow condition.

2.3 Flow conditions

In single-phase flow experiments, the range of

Reynolds number, Re ($=\rho u D_h/\mu$), was 1 700 – 24 000. In two-phase flow experiments, the ranges of the volumetric fluxes of water and air for the whole channel were $0.1 \leq j_L \leq 2.0$ m/s and $0.1 \leq j_G \leq 20$ m/s. Flow patterns observed were bubble flow, slug or churn flow and annular flow.

3. Results and Discussion

3.1 Single-phase flow

3.1.1 Turbulent mixing rate data Figure 3 shows turbulent mixing rate data obtained from the single-phase flow experiments. The ordinate is the dimensionless mixing rate, W'/μ, and the abscissa the Reynolds number for the whole channel, Re. Here, μ is the dynamic viscosity. Data points are labeled according to the working fluids. No difference is seen between the mixing rates, W'/μ, of air and water within a scatter of the data. W'/μ increases with Re. The increment in W'/μ against Re is relatively small in $2\times10^3 < Re < 10^4$, while large in $Re > 10^4$. The reason of the difference in the increment is probably due to the difference in flow in the subchannels. That is, the flow in $2\times10^3 < Re < 10^4$ is considered to be in a transition region where laminar flow and turbulent flow alternately occur, while a fully developed turbulent flow in $Re > 10^4$. According to Chen and Todreas' criteria[7], Re_{bl} and Re_{bt}, at which the laminar-to-transition and the transition-to-turbulent occur, are respectively defined as the following correlations:

$$\log\left(\frac{Re_{bl}}{300}\right) = 1.7\left(\frac{p}{d} - 1.0\right) \text{ laminar-transition} \quad (2)$$

$$\log\left(\frac{Re_{bt}}{10\,000}\right) = 0.7\left(\frac{p}{d} - 1.0\right) \text{ transition-turbulent.} \quad (3)$$

In the upper side of Fig. 3, Re_{bl} and Re_{bt} calculated from Eqs. (2) and (3) are depicted. In addition, Re_{bl} from Yang's criterion[8] and Re_{bt} from Johannsen's one[9] are drawn in the lower side. The Re_{bl} in the present experiment agrees approximately with Yang's criterion, while the Re_{bt} with Chen and Todreas' criterion, Eq. (3).

Figure 4 shows the comparison of the present turbulent mixing rate data with those for triangle lattice rod bundle reported in literatures[10]–[13]. From the comparison, the complicated effects are noticed of channel size, e.g., the hydraulic diameter, D_h, the gap clearance, S_{ij}, the pitch to rod diameter ratio, p/d on W'. That is, W'/μ is different depending on the differences in those sizes. The present data lie on the lowest part.

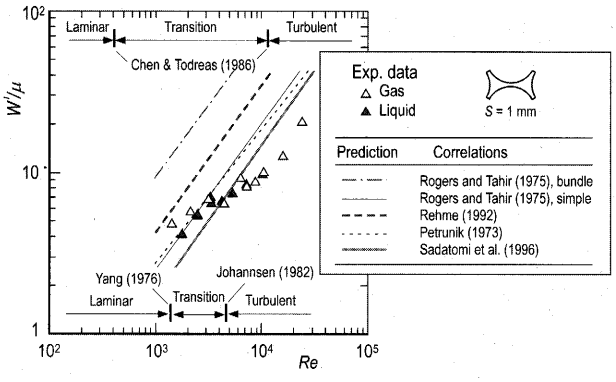

Fig. 3 Single-phase turbulent mixing rate data and the prediction of the several correlations

3.1.2 Assessment of correlations and models In this section, the applicability of the existing correlations and models for triangle lattice fuel rod bundles are assessed against the present data. The correlations and models are briefly introduced below.

Petrunik[10] proposed the next correlation based on his own data, which are shown in Fig. 4.

$$\frac{W'}{\mu} = 0.009 Re^{0.827}. \quad (4)$$

Rogers and Tahir[12] developed the following correlations for bundle and simple geometries:

$$\frac{W'}{\mu} = 0.005\,8\left(\frac{S_{ij}}{d}\right)^{-0.46} Re^{0.9} : \text{Bundle geometry} \quad (5)$$

$$\frac{W'}{\mu} = 0.001\,8\left(\frac{S_{ij}}{d}\right)^{-0.4} Re^{0.9} : \text{Simple geometry} \quad (6)$$

Rehme[14] obtained the following correlation from a number of experimental data for various square and triangular lattice bundles.

$$\frac{W'}{\mu} = 0.009\,21\left(\frac{1}{1+S_{ij}/d}\right) Re^{0.9}. \quad (7)$$

Sadatomi et al.[15] proposed a model, in which the turbulent mixing rate was calculated as the sum of two components, i.e., turbulent diffusion and convective transfer:

$$W' = W'_{TD} + W'_{CT}. \quad (8)$$

In Eq. (8), W'_{TD} is calculated from

$$W'_{TD} = \frac{\rho \varepsilon_D}{2F_i^*}, \quad (9)$$

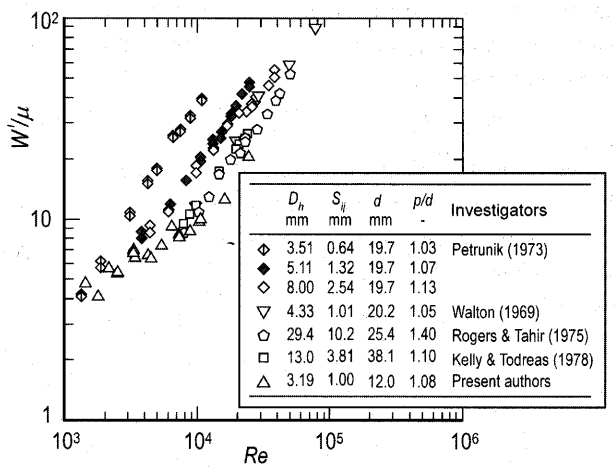

Fig. 4 Single-phase turbulent mixing rate data for several triangle lattice channels

where ρ is the density, ε_D the turbulent diffusivity and F_i^* the subchannel geometry factor. ε_D is calculated from Elder's equation[16]:

$$\varepsilon_D/\nu = 0.040 Re\sqrt{f}, \tag{10}$$

$$f = 0.079 Re^{-0.25}. \tag{11}$$

In Eq. (10), ν is the kinetic viscosity. The subchannel geometry factor, F_i^*, in Eq. (9) is calculated from

$$F_i^* = -\frac{1}{2}\sin^{-1}\left(\frac{p/d}{\sqrt{3}}\right) + \frac{p/d}{\sqrt{(p/d)^2-1}}\tan^{-1}\left[\frac{(p/d+1)\tan\left\{\frac{1}{2}\sin^{-1}\left((p/d)/\sqrt{3}\right)\right\}}{\sqrt{(p/d)^2-1}}\right] \tag{12}$$

for a triangle lattice rod bundle. W'_{CT} in Eq. (8) is calculated from

$$W'_{CT} = \beta_{CT} S_{ij} G, \tag{13}$$

where G is the mass flux, and β_{CT} the mixing Stanton number expressing the convective transfer effect:

$$\beta_{CT} = 0.000\,023 (S_{ij}/d)^{-1.86}, \tag{14}$$

for a triangle lattice rod bundle.

A comparison of the above correlations with the present data is also made in Fig. 3. The result shows that all the correlations over-predict the present data in $Re > 4\times10^3$.

Since no correlation could predict the present data, we tried to modify the Sadatomi et al.'s one. In the modification, instead of Blasius equation in Eq. (11), the following Chen and Todreas' correlation[7] was used:

$$f = f_l(1-\psi) + f_t\psi, \tag{15}$$

$$\psi = \frac{\log Re - \log Re_{bl}}{\log Re_{bt} - \log Re_{bl}} \tag{16}$$

ψ defined as Eq. (16) is called an intermittency factor. According to the description in section 3.1.1, Re_{bl} is taken as a constant value of 1 400, while Re_{bt} is calculated from Eq. (3). f_l and f_t in Eq. (15), the friction factors respectively for laminar and fully developed turbulent flows, are calculated from

$$f_l = C_l Re^{-1}, \quad f_t = C_t Re^{-0.25}. \tag{17}$$

C_l, the geometry factor for laminar flow in a triangular lattice rod bundle can be evaluated from Rehme's study[17]. C_t for fully developed turbulent flow can be calculated from Sadatomi et al.'s correlation[18] by substituting the above C_l.

$$\frac{C_t}{C_{t0}} = \sqrt[3]{0.015\,4\frac{C_l}{C_{t0}} - 0.012} + 0.85. \tag{18}$$

Here, C_{t0} and C_{l0} are the geometry factors for a circular channel, i.e., $C_{t0} = 0.079$ and $C_{l0} = 16$.

In order to obtain a new correlation of W'_{CT}, we evaluated the W'_{CT} by substituting the present W' data and the calculated value of W'_{TD} from Eq. (9) along with Eqs. (10), (12) and (15)–(18) into

$$W'_{CT} = W' - W'_{TD}. \tag{19}$$

In addition, we determined β_{CT} by substituting the above W'_{CT} into Eq. (13). Figure 5 shows β_{CT} data evaluated from the above procedure. β_{CT} decreases with increasing of Re in the laminar to fully developed turbulent transition region and is constant in the turbulent flow region. Therefore, by fitting the data, we obtained the following correlation:

$$\beta_{CT} = \beta_{CT,l}(1-\psi)^\gamma + \beta_{CT,t}\psi^\gamma. \tag{20}$$

Here, $\gamma = 1.3$, and $\beta_{CT,l}$ and $\beta_{CT,t}$ is respectively the mixing Stanton number at $Re = Re_{bl}$ and at $Re > Re_{bt}$. $\beta_{CT,l}$ was taken as a constant value of 0.007. On the other side, $\beta_{CT,t}$ was correlated from available W' data for various triangular lattice bundles[10)–13)].

$$\beta_{CT,t} = 0.000\,55\{1 + 1.3\times10^4 \exp(-33 S_{ij}/D_h)\}. \tag{21}$$

In Fig. 6, $\beta_{CT,t}$ data, obtained from Eqs. (9), (10), (12), (13), (15)–(19) and the W' data, are well correlated with Eq. (21) besides one data points by Petrunik[10].

Figure 7 shows the comparison of the present W' data with the present calculations, i.e., the sum of W'_{TD} (from Eqs. (9), (10), (12) and (15)–(18)) and W'_{CT} (from Eqs. (13), (20) and (21)). Good agreement was obtained between the calculations and the data in the transition region as well as the turbulent flow region. In order to confirm the validity of the present prediction method, we tested against the data for the above triangle lattice bundle[10)–13)]. Figure 8 (a) – (d) shows the test results. The present method can predict well the data by Walton[11], Rogers and Tahir[12], and Kelly and Todreas[13], irrespective of channel size, i.e., the hydraulic diameter, the gap clearance and the rod diameter etc., and a little underpredict the data by Petrunik[10].

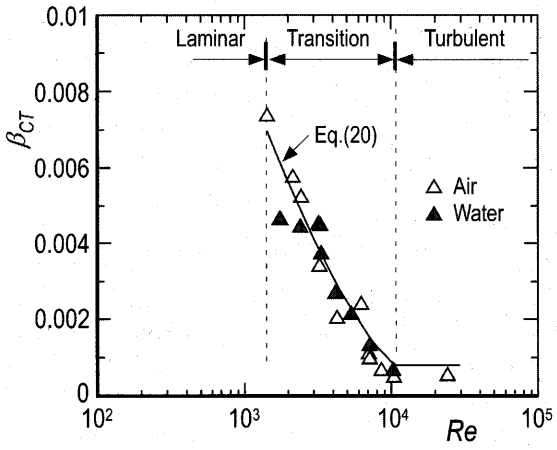

Fig. 5 Mixing Stanton number due to convective transfer for the present tight lattice subchannel

3.2 Two-phase flow

3.2.1 Effect of flow regime Figure 9 shows W'_k data obtained from the two-phase flow experiments. The data for the liquid and the gas are plotted against the superficial gas velocity, j_G, for the liquid velocity, j_L, as a parameter. The following characteristics are seen with the increase in j_G at a fixed j_L. In bubble flows, the liquid mixing rate, W'_L, solid symbol, is close to that of single-phase liquid flow at $j_G = 0$ and gradually increases with the approaching of bubble-slug transition point. In slug or churn flows, W'_L is about five times larger than that of the single-phase flow and decreases with the approaching

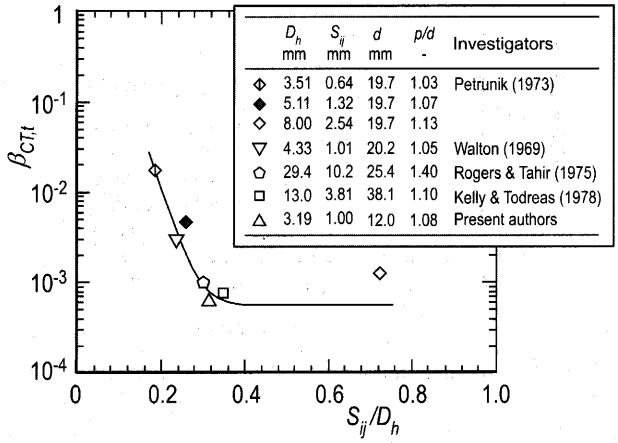

Fig. 6 Mixing Stanton number due to convective transfer for fully developed turbulent flow region in several triangle lattice channels

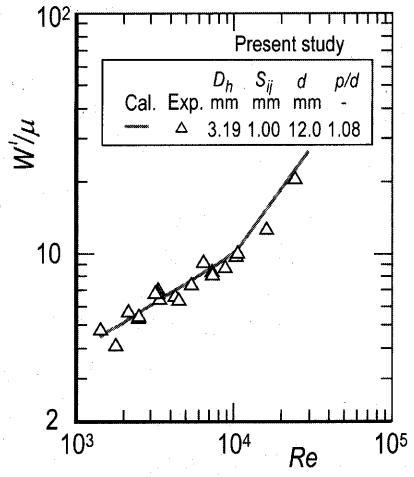

Fig. 7 Assessment results of the proposed prediction method against the present data

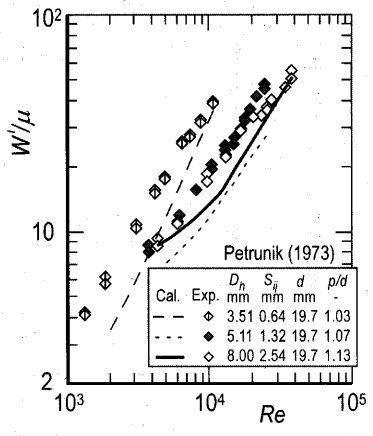

(a) Petrunik

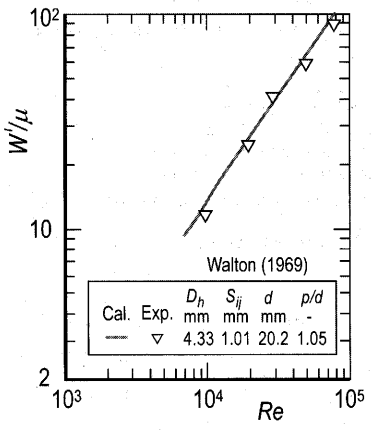

(b) Walton

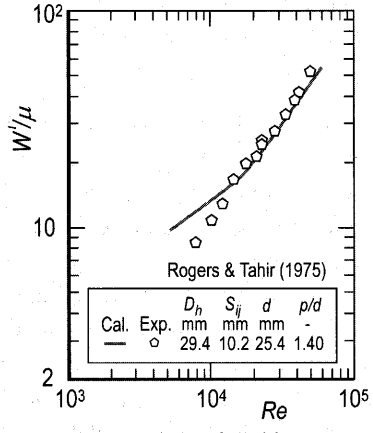

(c) Rogers & Tahir

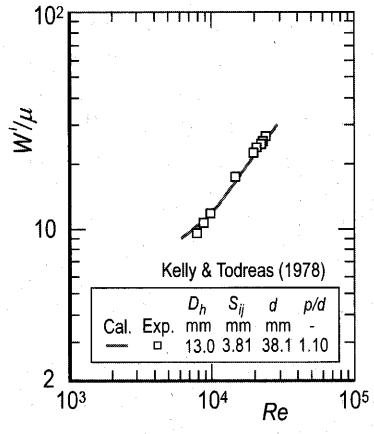

(d) Kelly & Todreas

Fig. 8 Assessment results of the proposed prediction method against several triangular lattice subchannel data

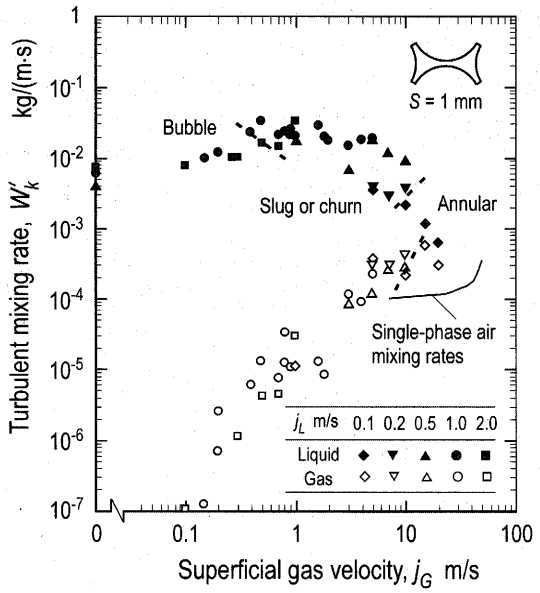

Fig. 9 Two-phase turbulent mixing rates data for tight lattice subchannel

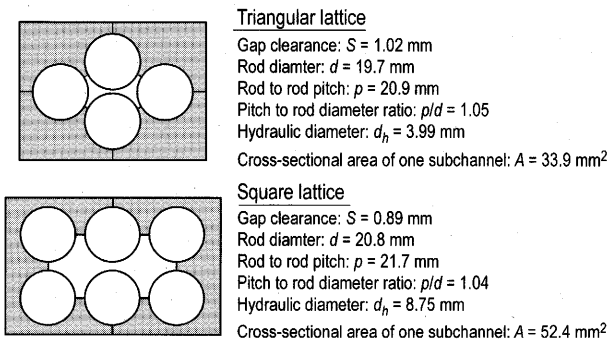

Fig. 10 Cross-sections of Rudzinski et al.'s test sections[22]

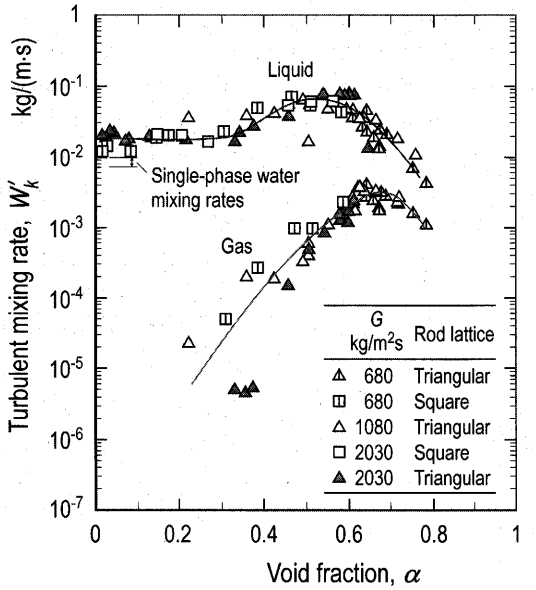

Fig. 11 Turbulent mixing rates data by Rudzinski et al.[22]

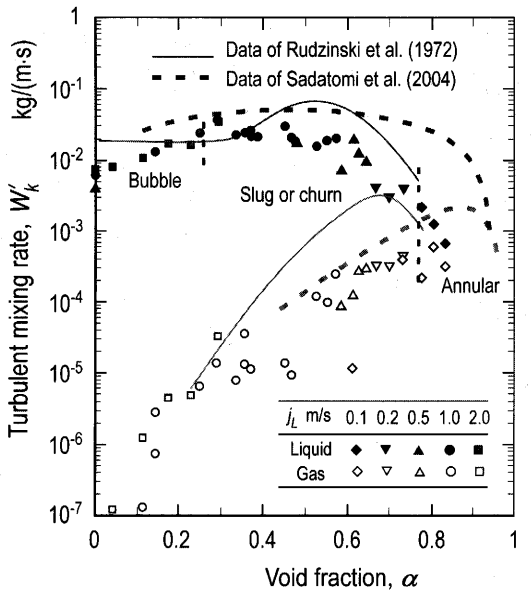

Fig. 12 Comparison of the turbulent mixing rates among several channels

of churn-annular transition point. In annular flows, W'_L decreases monotonically with the increase in j_G. On the other side, the gas phase mixing rate, W'_G, open symbol, is about zero for bubble flows. In slug or churn flows, W'_G drastically increases with j_G. In annular flows, W'_G tend to approach to a line corresponding to the mixing rate of the single-phase air flow. Such a flow pattern dependency is similar to that observed for square lattice channel as well as simple channels in our previous studies[6),(19)–(21)].

3.2.2 Effect of size and/or geometry of subchannel In order to see the effects of the size and/or geometry of subchannel on W'_k, the present data were compared with those of Rudzinski et al.[22] Figure 10 shows the cross-sections of their test channels. The gap clearances of these channels are about 1 mm, being similar to that of ours. The hydraulic diameter and cross-sectional area of the subchannel in their triangular lattice channel are respectively 1.25 and 2 times larger than ours, while in their square one 2.7 and 3.2 times larger. Figure 11 shows Rudzinski et al.'s W'_k data, obtained at about 0.34 MPa (absolute) using air-water as the working fluids. Though the abscissa in the original paper[22] was quality, it was replaced in Fig. 11 by void fraction, α, calculated from an empirical correlation for the present channel to facilitate comparison with the present data. Their data appear to be well represented by two solid curves for the liquid and gas phases, irrespective of the rod lattice and the mass velocity, G. To compare the present W'_k data with Rudzinski et al.'s data, the same curves are drawn on Fig. 12. The trend of W'_k against α is qualitatively the same between the Rudzinski et al.'s and the present data, but not quantitatively. That is, the W'_k for both phases is much smaller in the present channel than the Rudzinski et al.'s one, especially for slug or churn flow and annular flows in the void

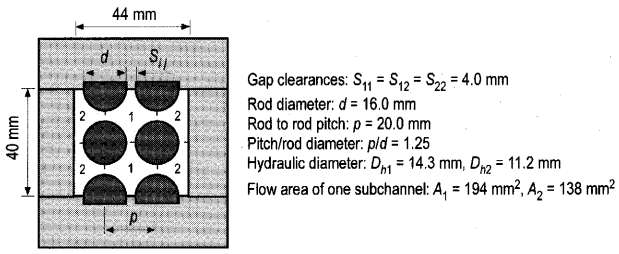

Fig. 13 Cross-section of Sadatomi et al.'s 2×3 rod channel[21]

fraction range of $\alpha > 0.4$. Two broken lines are also drawn on Fig. 12. These represent our air-water data[21] obtained between two central subchannels in a 2×3 rod channel simulating square lattice BWR fuel rod bundle shown in Fig. 13. The hydraulic diameter and cross-sectional area of Ch.1 is 4.5 and 12 times larger than those of the present triangle lattice channel. The turbulent mixing rate is much larger in the 2×3 rod channel than the present channel, especially for the liquid phase. One reason why the turbulent mixing rate is smaller in the present channel than the other channels is presumably due to the reduction in turbulence in the present channel. The turbulent mixing rate in two-phase flows has been considered to be the sum of the three components of turbulent diffusion, convective transfer and pressure difference fluctuations between subchannels[19),(20)]. Regarding the Reynolds numbers in the respective channels under the same mass flux condition, the Reynolds number is smaller in the present tight lattice subchannel than the other channels because of the smaller hydraulic diameter. Thus, the turbulent diffusion component becomes smaller in the present channel since turbulence becomes weaker with the decrease in Reynolds number.

As for the channel size effect on two-phase flow characteristics, it is reported that the effect appears in a capillary channel with hydraulic diameters of the order of, or smaller than, the following Laplace constant[23],

$$La = \sqrt{\frac{\sigma}{g(\rho_L - \rho_G)}}, \tag{22}$$

where σ is the surface tension, g is the gravitational acceleration. This length scale gives a criterion to determine whether two-phase flow is dominated by surface tension force. For the present air-water flow under atmospheric pressure and room temperature conditions, La is around 2.7 mm, which is close to 3.19 mm, the hydraulic diameter of the present tight lattice subchannel. As a result, it can be said that the channel size, e.g., the hydraulic diameter and cross-sectional area, significantly affects the two-phase turbulent mixing rate. Therefore, any prediction model of the mixing rate should include the channel size effects.

3.2.3 Assessment of correlation In this section, the latest correlation of Carlucci et al.[24] is assessed against the present two-phase flow data. Carlucci et al.[24]

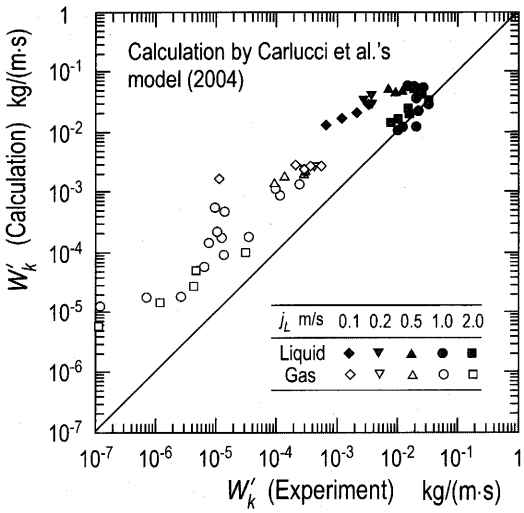

Fig. 14 Comparison of two-phase turbulent mixing rates between the present experiment and the calculation by Carlucci et al.'s model[24]

developed a new correlation, on the basis of observations by Rowe and Angle[25], Rudzinski et al.[22], Sadatomi et al.[6] and Kawahara et al.[20] In the correlation, the two-phase mixing rates are the sum of a homogeneous mixing rate and an additional mixing rate resulting from flow regime enhancement effects:

$$W'_L = W'_{L,\mathrm{hom}} + \Delta W'_{L,2\phi}, \quad W'_{L,\mathrm{hom}} = (1-x)W'_{\mathrm{hom}}. \tag{23}$$

$$W'_G = W'_{G,\mathrm{hom}} + \Delta W'_{G,2\phi}, \quad W'_{G,\mathrm{hom}} = xW'_{\mathrm{hom}}. \tag{24}$$

The homogeneous mixing rate, W'_{hom}, for a triangle lattice is calculated from Rogers and Tahir's correlations[12], Eq. (6), with a mixture Reynolds number, Re_m, and a homogeneous viscosity, μ_{hom}:

$$Re_m = \frac{(G_G + G_L)D_h}{\mu_{\mathrm{hom}}}, \quad \mu_{\mathrm{hom}} = \left(\frac{x}{\mu_G} + \frac{1-x}{\mu_L}\right)^{-1}. \tag{25}$$

The additional mixing rate, $W'_{k,2\phi}$, is calculated from

$$\Delta W'_{L,2\phi} = 0.051\,5 \exp\left\{-0.5\left(\frac{\alpha - 0.53}{0.179\,4}\right)^2\right\}, \tag{26}$$

$$\Delta W'_{G,2\phi} = 0.002\,64 \exp[-8.332\{\ln(1 - 1.9412(\alpha - 0.758\,84))\}^2]. \tag{27}$$

Equations (26) and (27) were obtaining by fitting data of Rudzinski et al.[22] for triangular lattice channel as well as square one.

Figure 14 shows assessment results of Carlucci et al.'s model against the present data. Their model roughly ten times over-predicts the present data, especially for slug or churn flow and annular flow regions. The reason of the over-prediction is that the Carlucci et al.'s model was based on the Rudzinski et al.'s mixing rates, being larger than those of the present channel, as described in section 3.2.2. Thus, there is a room for improvement in their model by accounting for channel size effects.

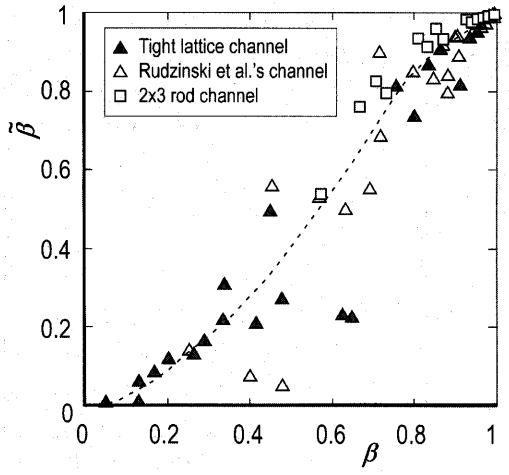

Fig. 15 Relation of gas volumetric flow fraction between axial and lateral directions

3.2.4 Relationship between gas and liquid turbulent mixing rates In two-phase flows, W'_L and W'_G are not independent of each other. Thus, one of them is expected to be determined from the other through a gas volumetric flow fraction of lateral flow, $\tilde{\beta}$[20),(26)], defined as

$$\tilde{\beta} = \tilde{V}_G/(\tilde{V}_G + \tilde{V}). \tag{28}$$

Here, $\tilde{V}_G$ and $\tilde{V}_L$ are the lateral volumetric fluxes of gas and liquid phases due to the turbulent mixing:

$$\tilde{V}_G = W'_G/(\rho_G S_{ij}), \quad \tilde{V}_L = W'_L/(\rho_L S_{ij}). \tag{29}$$

Figure 15 compares $\tilde{\beta}$ data for the present triangle tight lattice channel, Rudzinski et al.'s triangle lattice channel and Sadatomi et al.'s square lattice channel. The data are plotted against the following gas volumetric flow fraction of axial flow,

$$\beta = j_G/(j_G + j_L). \tag{30}$$

Here, j_G and j_L are the volumetric fluxes of gas and liquid in the channel, respectively. There is a unique relationship between $\tilde{\beta}$ and β, irrespective of channel size and rod lattice, though the scatter of the data exists depending on the inaccuracies of W'_G and W'_L data. This relationship seems useful to predict one of W'_G and W'_L if the other of them could be well predicted.

4. Conclusions

In order to obtain data on the turbulent mixing rate between triangle tight lattice subchannels, adiabatic air-water experiments were conducted for single- and two-phase flows under hydrodynamic equilibrium flow conditions. By analyzing the data, we found the followings:

- For single-phase turbulent mixing rate, a new prediction method was developed by modifying Sadatomi et al.'s model[15]. The method could predict well the present data as well as the data for several triangle lattice channels in literatures.
- The two-phase turbulent mixing rates in the present experiments were considerably smaller than those for our square lattice channel and Rudzinski et al.'s square and triangle lattice channels, i.e., a channel size effect was observed.
- Carlucci et al.'s model[24] over-predicted the present two-phase mixing rate data.
- A unique relationship of $\tilde{\beta}$ and β, gas volumetric flow fractions for the lateral flow and the axial flow, held irrespective of the rod lattice and the channel size.

As a future study, we are planning to conduct a similar experiment using air and low surface tension liquid as working fluids. The reason are (I) in an actual BWR, the working fluids are steam and water under high pressure and temperature condition, and the surface tension for the fluids is much lower than that for air and water; and (II) it is known that the reduction of surface tension leads to the reduction bubble size in bubble flows and the reduction of roughness in liquid film in annular flows, and thus may affect the turbulent mixing phenomena. Also, a similar experiment will be needed in a multi-subchannel system[21),(27)], which is close to an actual tight lattice fuel rod bundle because it is important to know that the results from the experiment in the present two-subchannel system are applicable to the prediction of flow characteristics in the multi-subchannel system.

Acknowledgments

The authors wish to express gratitude to Messrs. Y. Kimura and M. Mori for their experimental cooperation, and to the Institute of Applied Energy (IAE) and Ministry of Economy, Trade and Industry (METI) for providing financial support to this work.

References

(1) Iwamura, T., Okubo, T., Kureta, M., Nakatsukasa, T. and Takeda, R., Development of Reduced-Moderation Water Reactor (RMWR) for Sustainable Energy Supply, Proc. of 13th Pacific Basin Nuclear Conference, (2002), pp.1631–1637.

(2) Lahey, Jr., R.T. and Moody, F.J., The Thermal-Hydraulics of a Boiling Water Nuclear Reactor, 2nd ed., (1993), ANS, La Grange Park.

(3) Sadatomi, M., Kawahara, A. and Sato, Y., Lateral Velocities Due to Diversion Cross-Flow and Void Drift in a Hydraulically Non-Equilibrium Two-Phase Subchannel Flow, Proc. of 1997 ASME Fluids Eng. Division Summer Meeting, FEDSM'97, (1997), 7 pages in CD-ROM.

(4) Kawahara, A., Sadatomi, M., Kano, K. and Sasaki, Y., Flow Redistribution Due to Void Drift in Triangle Tight Lattice Subchannels, Proc. of Int. Conf. of Multiphase Flow ICMF2004, Paper No.223, (2004), 14 pages in CD-ROM.

(5) Kawahara, A., Sadatomi, M., Kano, K., Sasaki, Y. and Kudo, H., Void Diffusion Coefficient in Two-Phase

Void Drift for Several Channels of Two-and Multi-Subchannel Systems, Proc. of Japan-US Seminar on Two-Phase Flow Dynamics, Vol.1 (2004), pp.157–166.
(6) Sadatomi, M., Kawahara, A. and Sato, Y., Turbulent Mixing of Both Gas and Liquid Phases between Subchannels in Two-Phase Hydrodynamic Equilibrium Flows, Proc. Int. Symposium on Two-Phase Flow Modelling and Experimentation 1995, Vol.1, Edited by Celeta, G.P. and Shah, R.K., (1995), pp.403–409.
(7) Chen, S.K. and Todreas, N.E., Hydrodynamic Models and Correlations for Bare and Wire-Wrapped Hexagonal Rod Bundles—Bundle Friction Factors, Subchannel Friction Factors and Mixing Parameters, Nucl. Eng. Des., Vol.92 (1986), pp.227–251.
(8) Yang, J.W., A Note on Turbulent-Laminar Transition for Flow in Triangular Rod Bundles, Nucl. Sci. Engrg., Vol.62 (1976), pp.579–582.
(9) Johannsen, K., Longitudinal Flow over Tube Bundle, Low Reynolds Number Flow Heat Exchangers, Edited by Kakac, S., Shah, R.K. and Bergles, A.E., (1982), Hemisphere Pub. Co., New York.
(10) Petrunik, K., Turbulent Interchange in Simulated Rod Bundle Geometries for Genetron-12, Ph.D. Thesis, Dept. of Chemical Engineering, University of Windsor, Canada, (1973).
(11) Walton, F.B., Turbulent Mixing Measurements for Single Phase Air, Single Phase Water and Two-Phase Air Water Flows in Adjacent Triangular Subchannels, MS Thesis, Chemical Engineering, University of Windsor, Canada, (1969).
(12) Rogers, J.T. and Tahir, A.E.E., Turbulent Interchange Mixing in Rod Bundles and the Role of Secondary Flows, ASME Paper, No.75-HT-31, (1975).
(13) Kelly, J.M. and Todreas, N.E., Turbulent Interchange in Triangular Array Bare Rod Bundles, Proc. of 6th Int. Heat Transfer Conference, Toronto, Canada, Vol.5 (1978), pp.11–16.
(14) Rehme, K., The Structure of Turbulence in Rod Bundles and the Implication on Natural Mixing between the Subchannels, Int. J. Heat Mass Transfer, Vol.35 (1992), pp.567–581.
(15) Sadatomi, M., Kawahara, A. and Sato, Y., Prediction of Single-Phase Turbulent Mixing Rate between Two Parallel Subchannels Using a Subchannel Geometry Factor, Nucl. Eng. Des., Vol.162 (1996), pp.245–256.
(16) Elder, J.W., The Dispersion of Marked Fluid in Turbulent Shear Flow, J. Fluid Mech., Vol.5 (1959), pp.242–249.
(17) Rehme, K., Pressure Drop Performance of Rod Bundles in Hexagonal Arrangements, Int. J. Heat Mass Transfer, Vol.16 (1973), pp.933–950.
(18) Sadatomi, M., Sato, Y. and Saruwatari, S., Two-Phase Flow in Vertical Noncircular Channels, Int. J. Multiphase Flow, Vol.8 (1982), pp.641–655.
(19) Kawahara, A., Sato, Y. and Sadatomi, M., The Turbulent Mixing Rate and the Fluctuations of Static Pressure Difference between Adjacent Subchannels in a Two-Phase Subchannel Flow, Nucl. Eng. Des., Vol.175 (1997), pp.97–106.
(20) Kawahara, A., Sadatomi, M., Tomino, T. and Sato, Y., Prediction of Turbulent Mixing Rates of Both Gas and Liquid Phases between Adjacent Subchannels in a Two-Phase Slug-Churn Flow, Nucl. Eng. Des., Vol.202 (2000), pp.27–38.
(21) Sadatomi, M., Kawahara, A., Kano, K. and Sumi, Y., Single-and Two-Phase Turbulent Mixing Rate between Adjacent Subchannels in a Vertical 2×3 Rod Array Channel, Int. J. Multiphase Flow, Vol.30 (2004), pp.481–498.
(22) Rudzinski, K.F., Singh, K. and St. Pierre, C.C., Turbulent Mixing for Air-Water Two-Phase Flows in Simulated Rod Bundle Geometry, Can. J. Chem. Eng., Vol.50 (1972), pp.297–299.
(23) Triplett, K.A., Ghiaasiaan, S.M., Abdel-Khalik, S.I. and Sadowski, D.L., Gas-Liquid Two-Phase Flow in Microchannels—Part I: Two-Phase Flow Patterns, Int. J. Multiphase Flow, Vol.25 (1999), pp.377–394.
(24) Carlucci, L.N., Hammouda, N. and Rowe, D.S., Two-Phase Turbulent Mixing and Buoyancy Drift in Rod Bundles, Nucl. Eng. Des., Vol.227 (2004), pp.65–84.
(25) Rowe, D.S. and Angle, C.W., Crossflow Mixing between Parallel Flow Channels during Boiling—Part 3: Effect of Spacers on Mixing between Two Channels, Pacific Northwest Laboratory Rep. BNWL-371 Pt. 3, (1969).
(26) Kawahara, A., Sadatomi, M. and Sato, Y., Turbulent Mixing of both Gas and Liquid Phases between Adjacent Subchannels in a Two-Phase Annular Flow, Proc. of Third Int. Conf. on Multiphase Flow ICMF'98, (1998), 8 pages in CD-ROM.
(27) Sadatomi, M., Kawahara, A., Kano, K. and Tanoue, S., Flow Characteristics in Hydraulically Equilibrium Two-Phase Flows in a Vertical 2×3 Rod Bundle Channel, Int. J. Multiphase Flow, Vol.30 (2004), pp.1093–1119.